Thermolysis mechanism of chromium nitrate nonahydrate and computerized modeling of intermediate products

P. Melnikov · V. A. Nascimento · I. V. Arkhangelsky · L. Z. Zanoni Consolo · L. C. S. de Oliveira

Abstract Thermal decomposition of chromium nitrate nonahydrate was studied by thermal analysis, differential scanning calorimetry, infrared spectroscopy, and high temperature X-ray diffraction, so that mass losses were related to the exactly coincident endothermic effects and vibrational energy levels of the evolved gases. The thermal decomposition of chromium nitrate is a complex process, which begins with the simultaneous dehydration and concurrent condensation of 4 mol of the initial monomer $Cr(NO_3)_3 \cdot 9H_2O$. Soon after that, the resulting product $Cr_4N_{12}O_{36} \cdot 31H_2O$ gradually loses water and azeotrope $HNO_3 + H_2O$, and is transformed into tetrameric oxynitrate $Cr_4N_4O_{16}$. At higher temperatures, the tetramer loses N_2O_3 and O_2 and a simultaneous oxidation of Cr(III) to Cr(IV) occurs. The resulting composition at this stage is chromium dioxide dimer Cr_4O_8. Finally, at 447 °C the unstable dimer loses oxygen and is transformed into $2Cr_2O_3$. The models of intermediate amorphous compounds represent a reasonably good approximation to the real structures and a proper interpretation of experimental data.

Keywords Chromium nitrate · Thermal decomposition · Computer modeling

P. Melnikov (✉) · V. A. Nascimento · L. Z. Zanoni Consolo
School of Medicine, Federal University of Mato Grosso do Sul, Caixa Postal 549, Campo Grande, MS, Brazil
e-mail: petrmelnikov@yahoo.com

I. V. Arkhangelsky
School of Chemistry, Moscow State University, Vorobievy Gory, 119517 Moscow, Russia

L. C. S. de Oliveira
School of Chemistry, Federal University of Mato Grosso do Sul, Caixa Postal 546, Campo Grande, MS, Brazil

Introduction

In a series of recently published papers concerning gallium [1], yttrium [2], aluminum [3], and gadolinium [4] nitrates, we reported on the most probable and simple mechanisms of their thermal decomposition. It was shown that except for $Al(NO_3)_3 \cdot 8H_2O$, the process starts with a simultaneous condensation of 4 mol of $Me(NO_3)_3 \cdot 9H_2O$. Soon after that, the resulting tetrameric heterocycle gradually loses water, nitric acid, and nitrogen oxides and through the formation of unstable oxynitrates are converted into Me_2O_3. In the case of aluminum nitrate, only two initial monomers are condensed giving rise to a smaller cycle $Al_2O_2(NO_3)_2$, which at higher temperature is also transformed into metal oxide. In all instances, the mass losses at the intermediate steps were shown to be in perfect agreement with the mechanisms proposed and the structural arrangements of the intermediate products.

Despite similarities with coordination chemistry of the aforementioned nitrates, the thermal decomposition of chromium nitrate is, in principle, a more complex process due to the variability of chromium valence states (II–VI) and the possibilities of oxygen insertion into the crystal lattice of chromium oxides. A number of compositions have been proposed as candidates for the intermediate oxycompounds, including $Cr_2O_3 \cdot 2CrO_3$, $Cr_2O_3 \cdot CrO_3$, CrO_2, $Cr(OH)_x(NO_3)_{3-x} \cdot yH_2O$, $CrO_{1.5+y}$ and others [5–7]. However, the physical presence of these oxides has never been proved beyond reasonable doubt owing to their amorphous character. Furthermore, the analytical procedures claimed to determine Cr(VI) [5] content in reality are not specific covering all oxidizing species, including Cr(IV) and non-stoichiometric oxides. The only positively identified CrO_2 X-ray diagram with rutile structure refers to the conditions comparable to those used in catalyst preparations

(thin films) [8]. As for Infrared spectroscopy (IR spectra), the co-existence of chromium-containing groups and NO_3^- bands overlapping the bands of the decomposition products creates a complex pattern which makes the interpretations unpracticable. In any case, no realistic mechanism has been proposed so far that fitted the events observed in thermo-analytical curves.

Since X-ray data are unavailable for most of the intermediate products and IR spectra of solids do not help much, additional tools are needed to deal with the identification of amorphous compounds. So we have chosen the molecular mechanics method to build up feasible models of unstable compounds forming during $Cr(NO_3)_3 \cdot 9H_2O$ thermolysis. Recently progress has been made toward the development of force fields that allow calculations of the minimal potential energy of these compounds and toward making (with due caution) a comparison of the stabilities of what we regard as the true intermediate oxynitrates. The purpose of this study is to apply the hypothesis supposing the nonahydrate condensation for a plausible interpretation of the experimental results.

Materials and methods

The starting reagent used was chromium nitrate nonahydrate $Cr(NO_3)_3 \cdot 9H_2O$, of analytical grade purity purchased from Sigma–Aldrich. Direct heating of the commercial reagent resulted in mass loss of 79.87 % confirming the water number of nine (calc. value 81.0 %).

Thermal gravimetric analysis (TG) and differential scanning calorimetry (DSC) were used to study thermal behavior, in both cases employing a Netsch STA Jupiter 449C Instrumentation. Test specimens of the starting material were heated in a flux of argon (50 mL min^{-1}, 99.998 % purity; oxygen content <5 ppm) in a 30–500 °C temperature range, at a heating rate of 10 °C min^{-1}. Mass losses during heatings were analyzed and compared to previously calculated values. Melting point was determined by capillary method, which relies on a visual detection of melt. The evolution of volatiles was measured using a Netsch STA Jupiter 449C. Infrared spectroscopy of evolved gases was performed using a Tensor 27 Bruker spectrometer. The spectra were detected in a 700–4,000 cm^{-1} range. Temperature of the transport gas line was 240 °C. The spectra were taken for 12 s at a frequency accuracy of 1 cm^{-1}. The identification of the IR spectra was done on the basis of NIST Chemistry WebBook [9].

X-ray diffraction (XRD) was carried out at the Brazilian synchrotron light laboratory (LNLS) at the D10B-XPD beam line. The line is equipped with a 4 + 2 circles Huber diffractometer placed at 13 m from the double crystal Si(111) monochromator [10]. The beam line end station

was configured so that a whole diffraction pattern ($10 < 2\theta < 90$) could be collected in at least 5 min intervals using a solid state Mythen 1 K detector that was placed in the two arm located 1 m after the sample. In all experiments the photon energy was fixed at 8.0 keV ($\lambda = 1.55064$ Å). In situ heating of the sample was obtained using a furnace specially designed for diffraction experiments. The heating rate used was 10 °C min^{-1} to simulate the conditions chosen for thermal analysis.

Compounds were simulated using the standard software package AVOGADRO, an open-source molecular builder and visualization tool, version 1.0.3. with the UFF force fields program [11, 12]. Structures were found by minimizing the energy with respect to all geometrical variables, no assumptions being made other than that of appropriate symmetry. Angles and interatomic distances were evaluated using special features of the program.

Results and discussion

Thermal analysis

As established by visual observations in air, the compound becomes liquid at around 55 °C. Then, this liquid starts to boil and, at ∼130 °C, the smell of HNO_3 fumes begins to be perceived. At higher temperatures, a foam-like black product with metallic luster is formed, slowly changing its color to dark green.

The TG and DSC curves of $Cr(NO_3)_3 \cdot 9H_2O$ are illustrated in Figs. 1 and 2. It is to be stressed that their form and resolution power strongly depends on applied atmosphere, sample mass and, above all, on heating rate. The patterns presented below are characteristic for the heating rate of 10 °C min^{-1} in argon flux.

It is well known that the decomposition onset for the nitrates of transition metals is generally below 100 °C due to a back-donation of electrons from the nitrate ions to an unfilled d-orbital of the cations [13, 14]. In this respect,
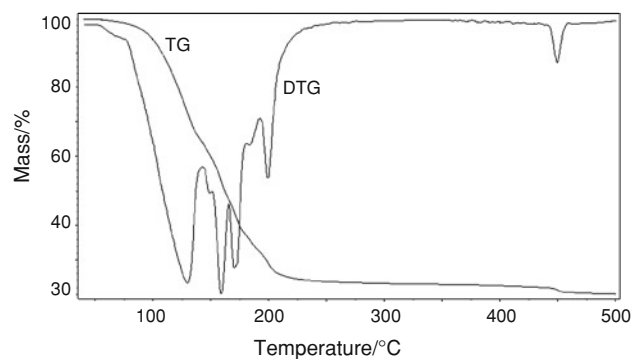

Fig. 1 TG and DTG curves of $Cr(NO_3)_3 \cdot 9H_2O$

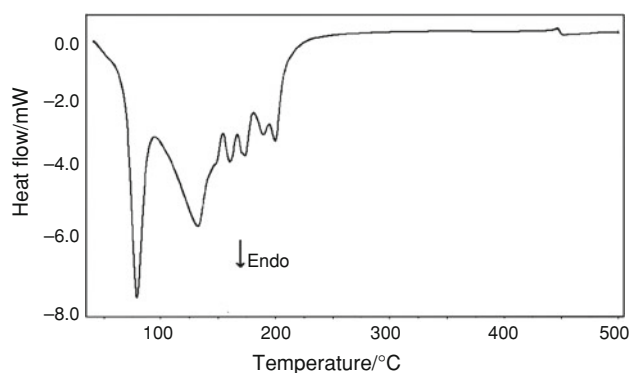**Fig. 2** DSC curve of $Cr(NO_3)_3 \cdot 9H_2O$

chromium nitrate is an analog of these elements. According to the TG and DSC curves, it melts in its own water of crystallization at 45 °C and, between 45 and 80 °C, loses $3.36 + 2.24 = 5.6$ % of mass. The largest loss of mass (61.37 %) takes place between 80 and 138 °C. The next loss of mass (11.07 %) occurs between 138 and 300 °C. Thus, total loss of volatile products amounts to 80.54 % matching the calculated value of 81 %. It can be seen that this loss really fit the values calculated for the formation of final Cr_2O_3 (Table 1).

It is understandable that the loss of mass which takes place during the first three stages, a total of 61.37 %, cannot physically result from the disintegration of the single mol of $Cr(NO_3)_3 \cdot 9H_2O$, if only because it possesses no more than one atom of metal, whereas at least two are required for the formation of Cr_2O_3 at the end of the process. Hence, one must take into consideration the process of condensation, characteristic of the chemistry of cations with the charge $+3$.

Here, it is worth referring to the existing published data on the elements, properties of which are close to chromium. For gallium, yttrium, gadolinium, and scandium, for example, it has been shown that such condensation leads to the formation of stable groups containing four metal atoms [1, 2, 4, 15]. As to chromium itself, tetrameric cyclic

Table 1 Mass losses at different stages of $4Cr(NO_3)_3 \cdot 9H_2O$ thermal decomposition in relation to the initial sum of four initial monomers

Stage	Composition	Mass loss/mol				Mass loss/%	
		H_2O	HNO_3	N_2O_3	O_2	Calc.	Exp.
1	$4[Cr(NO_3)_3 \cdot 9H_2O]$	3	–	–	–	3.37	3.6
2	$Cr_4N_{12}O_{36} \cdot 33H_2O$	2	–	–	–	5.60	5.56
3	$Cr_4N_{12}O_{36} \cdot 31H_2O$	27	8	–	–	67.5	66.93
4	$Cr_4N_4O_{16}$	–	–	2	1	79.0	78.5
5	Cr_4O_8	–	–	–	1	81.0	80.54
	$2Cr_2O_3$						

Total: $32H_2O$, $8HNO_3$, $2N_2O_3$, $2O_2$

species (or clusters) containing Cr(III) have been described long ago at advanced steps of hydrolytic polymerization [16]. Moreover, it was shown that these oligomers are relevant to protein binding in living organisms [17]. The main feature of chromium systems, however, is related to oxygen mobility with reversible redox processes.

Previous calculations show that the hypothesis concerning cluster pre-existence in the solid state is quite applicable to the present case of chromium nitrate nonahydrate. Indeed, that suggests that at least 4 mol of $Cr(NO_3)_3 \cdot 9H_2O$ are involved in the condensation process. Naturally, like in the instance of $Al(NO_3)_3 \cdot 6H_2O$ [3], we might start considering the condensation of $2[Cr(NO_3)_3 \cdot 9H_2O]$, but in this case, at the end of the process, we would have to resort to fractional values of stoichiometric coefficients for volatile products, and again address the need of further condensation.

However, the most probable option is that the clusters are formed at the stage of hydrolytic processes provoked by heating the molten nonahydrate at 50–80 °C. At the first and second stages, during the process of the initial melting and dehydration of the compound and immediately afterward, $3 + 2$ mol of loosely-bound water are removed which are partially consumed in subsequent hydrolysis. This produces a mass loss of: calc. 5.6 %; exp. 5.56 % with the formation of intermediate hydrate $Cr_4N_{12}O_{36} \cdot 33H_2O$ (Table 1).

At the third stage, 8 mol of HNO_3 and 27 mol of H_2O are removed, corresponding to total mass loss of: calc. 67.5 %; exp. 66.93 %. The removal of HNO_3 occurs in the form of the azeotrope with the composition 36.6 % H_2O–67.4 % HNO_3, and leads to the creation of oxygen bridges between the chromium atoms, obliging $4Cr(NO_3)_3$ to condense into a tetrameric structure $Cr_4O_4(NO_3)_4$. Simultaneously, the entire system of hydrogen bonds is destroyed. Both DTG and DSC curves show that this is a complex step-wise process, and the water evolved belongs differently bonded species.

At the fourth stage, tetramer loses 2 mol of N_2O_3 and 1 mol of oxygen with total mass loss 78.5 %, so the composition of the resulting solid product will correspond to Cr_4O_8. Finally, the latter will lose 1 mol of oxygen and be transformed into $2Cr_2O_3$ with total mass loss 80.54 %.

It is obvious that this scheme must be corroborated by additional experimental techniques.

Identification of volatile products

The 3D diagram of IR–spectrum shown in Fig. 3 gives a general view of absorption at sequential temperatures. It can be seen that the major gas evolution occurs near 100–160 °C, in accordance with the TG curve. The main mass loss up to 80 °C clearly correlates with the water
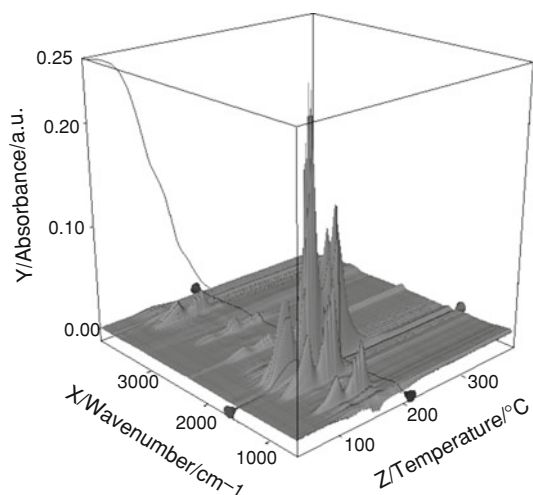
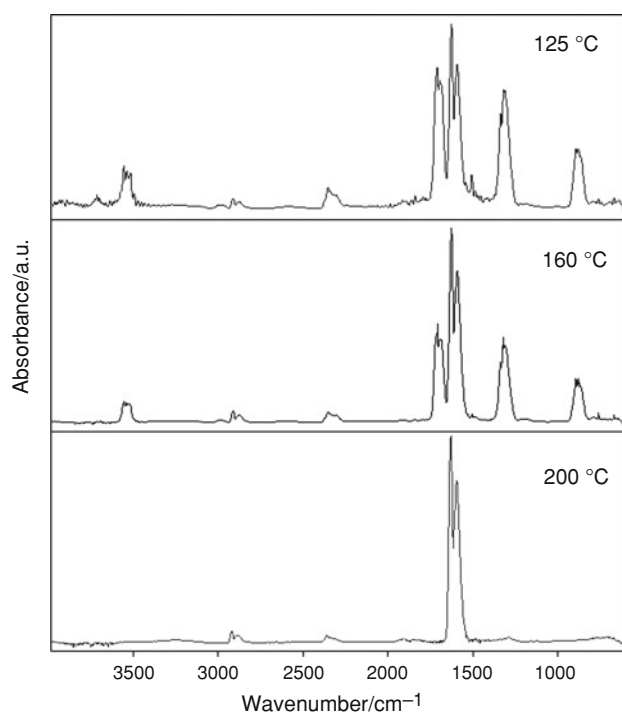**Fig. 3** Temperature-dependent 3D diagram of IR spectra of the $Cr(NO_3)_3 \cdot 9H_2O$ thermal degradation

Fig. 4 Profiles of the IR spectra corresponding to 125 and 160 and 200 °C

Fig. 5 Gram–Schmidt curve of the integrated spectral absorbance in relation to the TG and DSC curves

removal. Later on, significant contributions come from the water and nitric acid. The IR– spectrum of the sample corresponding to 160 °C (Fig. 4) confirms this suggestion by the presence of the main nitric acid absorbance bands at 762, 885, 1,508, 1,595, 1,630, 1,698, and 1,712 cm^{-1}.

According to the Gram–Schmidt curve, which describes integrated spectral absorbance, this effect starts at 120 °C (Fig. 5), exactly corresponding to the boiling point of the azeotrope [18].
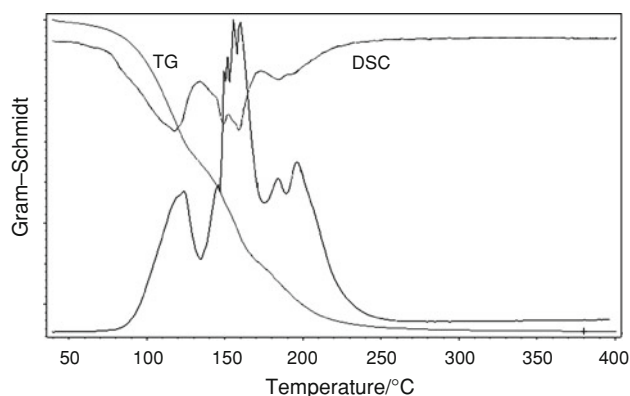
As one can see from IR absorbance profile at 200 °C (Fig. 4), the next mass loss is due to forming of nitrogen trioxide with the most significant characteristic bands at 1,314, 1,595, and 1,629 cm^{-1}. Since the mass loss at this stage is larger than that corresponding to 2 mol of N_2O_3, one can infer that another gaseous product is produced. Under these circumstances, oxygen is the only candidate with no changing dipole, so it is not detectable in IR spectrum. A possible mechanism in this case involves the nitrogen (V) reduction to $4NO_2$ with its conversion to $2N_2O_3$ and O_2. This process automatically implies the oxidation of Cr(III) to Cr(IV) as the difference in potentials N(V)–N(IV) would not permit the oxidation to chromate in solid state. Usually, this takes very aggressive oxidizing conditions in alkaline milieu to convert trivalent chromium to hexavalent [19]. Finally, the decomposition of chromium(IV) oxide produces 1 mol of oxygen and 2 mol of chromium trioxide.

Thus, the only volatile products of the whole process of $Cr(NO_3)_3 \cdot 9H_2O$ thermolysis are water, nitric acid, nitrogen trioxide, and oxygen. Returning to the Gram–Schmidt curve, one can see that it mirrors the DTG curve confirming that no other gaseous products are unaccounted for.

X-ray diffraction study

The 3D X-ray diagram obtained in situ is presented in Fig. 6. It can be seen that at temperature of 90 °C or probably lower original nitrate hydrate is completely transformed into amorphous material characterized by typical diffraction halos. This observation correlates with findings from other investigation techniques, the DSC curve in the first place (Fig. 2), with no exothermic effects which could be attributed to crystallization processes. The most interesting region of the diagram is given separately in Fig. 7 in the form of diffraction profiles corresponding to the range of 390–400 °C.
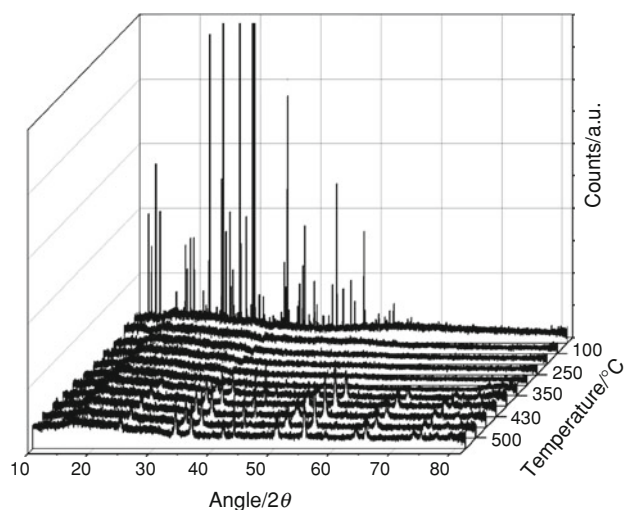
Fig. 6 3D high temperature X–ray diagram obtained in situ

According to the TG curve, at $\sim 380\ ^\circ$C chromium(IV) oxide should have been formed, though up to 390 $^\circ$C there are no signs of crystallization. This could be explained by poor diffusion and slow kinetics in the foam-like solid material. However, yet at 400 $^\circ$C, a clear diffraction pattern starts to appear showing the presence of Cr_2O_3 identified by the ICSD file 201102. The crystallization process goes along with the loss of oxygen as a result of chromium(IV) oxide decomposition. As expected, this loss of mass is accompanied by a small exothermic effect taking
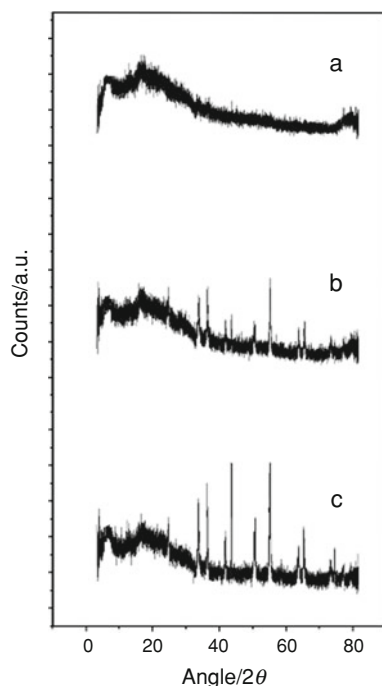

Fig. 7 Diffraction profiles corresponding to 390 (*a*), 400 (*b*) and 460 $^\circ$C (*c*)

place at 447 $^\circ$C. This temperature exactly corresponds to the phase transformation $CrO_2 \rightarrow Cr_2O_3$ described long ago [20], for pure crystalline chromium dioxide.

So, one fact still remains to be explained: why no researcher has been able so far to obtain crystalline CrO_2 by chromium nitrate decomposition? At this stage, the molecular modeling technique has been proven to be an effective tool.

Structural modeling

The models obtained using the molecular mechanics technique are shown in Figs. 8, 9, and 10. As can be seen from Figs. 8 and 9, the base of the tetramer is formed by an inorganic heterocycle composed of four atoms of chromium, alternating with four atoms of oxygen which, to simplify things, are numbered from 1 to 4. Together they form a rather symmetric crown-like cycle, wherein four chromiums and four oxygens sit in parallel planes, one anterior and the other posterior. In the projection (a), O(2) and O(4) are eclipsed by Cr(2) and Cr(3) while in the projection (b) the figure is staggered about the axis O(2)–O(4) in a way that the previously hidden oxygens have become clearly visible. The potential energy calculated for this structure is -11.42 kJ mol^{-1}. The corresponding interatomic distances and angles are given in Tables 2 and 3.

As one can see, four anions NO_3 are attached to yttrium atoms. It is evident that such arrangement admits the existence of a large population of conformers owing to the rotation about the bonds Cr–O and O–N, with the exception of the bridging O(1) and O(3). This model is relatively symmetric, but a number of intermediate asymmetric conformers can also exist, e.g., the extreme structure shown in Fig. 9. Strictly speaking, no conformational search routine guarantees that all conformers have been found. So we do not focus our attention on these isomers, because, in solid state, the rotational degrees of freedom are hindered or totally blocked due to the requirements imposed by the densest packing.

The interatomic distances and bond angles calculated using the UFF force fields program are presented in Tables 2 and 3. We can see that the heterocycle itself is symmetric as all distances Cr–O and angles Cr–O–Cr are identical: 1.897–1.898 Å and 104.40–104.60°, respectively. The comparison shows that the distances are of the same order as those refined from X-ray diffraction data for the high temperature modification of Cr_2O_3. i.e., in the range of 1.962–2.000Å (ICSD file 201102). The potential energy -9.61 kJ mol^{-1} for this structure is close to -11.42 kJ mol^{-1} which was previously calculated for a more symmetric arrangement.

As for NO_3 groups, they behave as normal nitrate anions with N–O distances 1.193 Å, that is very close to the interatomic distances in the NO_3^- groups of solid nitrates

Fig. 8 Tetramer model of symmetric rotamer $Cr_4N_4O_{16}$. **a**—O(2) and O(4) are eclipsed; **b**—O(2) and O(4) are visible

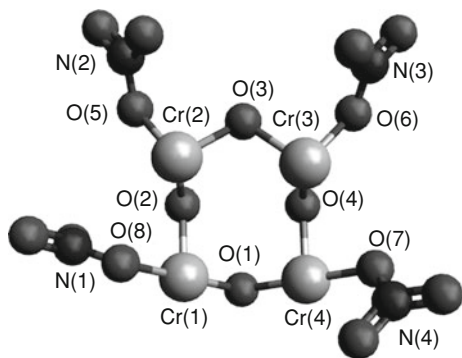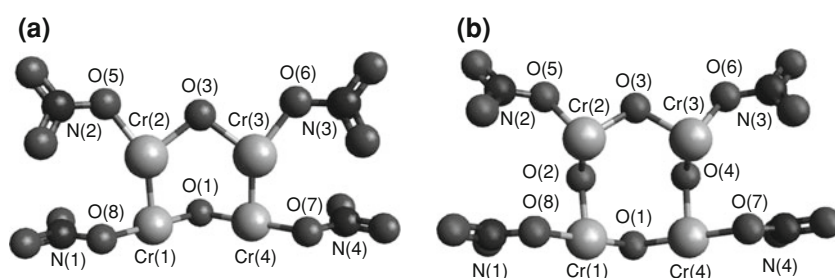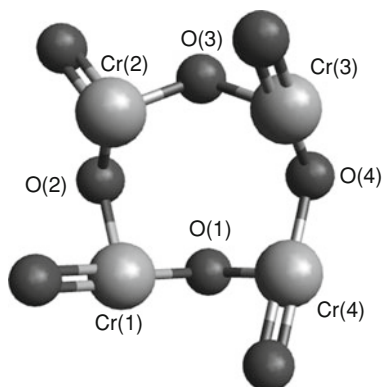**Fig. 9** Tetramer model of asymmetric rotamer $Cr_4N_4O_{16}$

Fig. 10 Tetramer model of Cr_4O_8

Table 2 Interatomic distances (Å) calculated for tetrameric models

Distances	$Cr_4O_4(NO_3)_4$	Cr_4O_8
Cr(1)–O(1)	1.898	1.898
Cr(1)–O(2)	1.898	1.898
Cr(2)–O(2)	1.898	1.898
Cr(2)–O(3)	1.898	1.898
Cr(3)–O(3)	1.897	1.898
Cr(3)–O(4)	1.897	1.898
Cr(4)–O(1)	1.898	1.898
Cr(4)–O(4)	1.898	1.898
Cr(1)–Cr(2)	3.001	3.001
Cr(1)–Cr(4)	3.000	3.001
Cr(2)–Cr(3)	2.998	3.001
Cr(3)–Cr(4)	3.001	3.001
N(1)–N(2)	4.064	–
N(1)–N(3)	9.103	–
N(2)–N(3)	7.739	–
N(2)–N(4)	9.071	
N(3)–N(4)	3.996	

Table 3 Bond angles (°) calculated for tetrameric models

Angles	$Cr_4O_4(NO_3)_4$	Cr_4O_8
Cr(1)–O(2)–Cr(2)	104.50	104.50
Cr(2)–O(3)–Cr(3)	104.40	104.50
Cr(3)–O(4)–Cr(4)	104.50	104.50
Cr(4)–O(1)–Cr(1)	104.60	104.50

established by X-ray methods (1.20–1.22 Å) [21]. Meanwhile, the bond angles O–N–O found for the model are identical to the angles in solid nitrates (all 120.00°) in accordance with the actual structure of the polyatomic ion, which has trigonal planar geometry [22].

Figure 10 shows the structure of the composition Cr_4O_8 that might be formed after the oxidation of Cr(III) to Cr(IV). Here, atoms numeration is the same as for the previous model. The comparison of the interatomic distances with those of $Cr_4O_4(NO_3)_4$ allows to state that they are practically identical. So, there is no contraction as it occurs in aluminum nitrate where they were drastically reduced in a smaller cycle [3]. In this case, no other conformation was found, so the arrangement must be rather stiff. The potential energy of -2.61 kJ mol^{-1} for this structure is of the same order of magnitude of the previous models.

The presence of this compound may explain the failure to detect the crystalline chromium dioxide during the thermal decomposition of chromium nitrate hydrate, because monomer CrO_2, at the moment of its formation at 447 °C, is transformed into $2Cr_2O_3$ with the evolution of spare O_2. Thus, all the aforementioned thermal effects and results of the instrumental methods are accounted for.

The complete decomposition process can be summarized as

$$4Cr(NO_3)_3 \cdot 9H_2O = 4Cr_2O_3 + 8HNO_3 + 4N_2O_3 + 2O_2 + 33H_2O$$
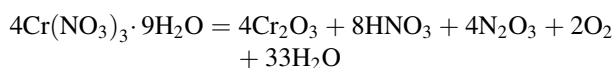
It is clear that the levels of potential energy, calculated by means of molecular mechanics do not necessarily have

any physical meaning in themselves. However, when considering a series of related structures, this method may be of help when interpreting the experimental findings of thermal analysis for intermediate amorphous compounds.

Conclusions

1. The thermal decomposition of chromium nitrate is a complex process, which begins with the dehydration and concurrent condensation of 4 mol of the initial monomer $Cr(NO_3)_3 \cdot 9H_2O$.

2. Soon after that, the resulting product $Cr_4N_{12}O_{36} \cdot 31H_2O$ gradually loses water and azeotrope $HNO_3 + H_2O$, and is transformed into tetrameric oxynitrate $Cr_4N_4O_{16}$.

3. At higher temperatures, the tetramer loses N_2O_3 and O_2 and a simultaneous oxidation of Cr(III) to Cr(IV) occurs. The resulting composition at this stage is chromium dioxide dimer Cr_4O_8.

4. Finally, at 447 °C, the unstable dimer loses oxygen and is transformed into $2Cr_2O_3$.

5. The models of intermediate amorphous compounds represent a reasonably good approximation to the real structures and a proper interpretation of experimental data.

References

1. Melnikov P, Nascimento VA, Zanoni Consolo LZZ. Thermal decomposition of gallium nitrate hydrate and modeling of thermolysis products. J Therm Anal Calorim. 2011;135:1117–21.

2. Melnikov P, Nascimento VA, Consolo LZZ, Silva AF. Mechanism of thermal decomposition of yttrium nitrate hexahydrate $Y(NO_3)_3 \cdot 6H_2O$ and modeling of intermediate oxynitrates. J Therm Anal Calorim. 2012. doi:10.1007/s10973-012-2236.

3. Melnikov P, Nascimento VA, Arkhangelsky IV, Zanoni Consolo LZZ. Thermal decomposition mechanism of aluminum nitrate octahydrate and characterization of intermediate products by the technique of computerized modeling. J Therm Anal Calorim. 2012. doi: 10.1007/s10973-012-2566-1.

4. Melnikov P, Nascimento VA, Consolo LZZ. Computerized modeling of intermediate compounds formed during thermal decomposition of gadolinium nitrate hydrate. Russ J Phys Chem. 2012;11:1659–63.

5. Gubrinowicz L, Strömich T. Study on the thermal decomposition of chromium(III) nitrate nonahydrate. Thermochim Acta. 1987; 115:137–51. (and references therein).

6. Hill WD. Chromium(IV) oxide prepared from chromium(III) nitrate nonahydrate. Inorg Chim Acta. 1982;65:L100.

7. Malecki A, Malecka B, Gajerski R, Labus S. Thermal decomposition of chromium(III) nitrate nonahydrate. J Therm Anal Calorim. 2003;72:133–44. (and references therein).

8. Maciejevski M, Köler K, Schjneider H, Baiker A. Interconversion of CrO_2 formed by decomposition of chromium nitrate nonahydrate. J Solid State Chem. 1995;119:13–23.

9. NIST Chemistry WebBook, NIST Standard Reference Database Number 69: www.http//webbook.nist/chemistry. Accessed 12 Dec 2012.

10. Robinson IK. Imaging of quantum array structures with coherent and partially coherent diffraction. J Synchrotron Rad. 2003;10: 409–15.

11. Young DC. Computational chemistry: a practical guide for applying techniques to real-world problems. New York: Wiley; 2001.

12. http://www.avogadro.openmolecules.net/. Accessed 21 Nov 2012.

13. Wesley WW, Roger GS. The fusion temperatures of the rare earth chloride and nitrate hydrates. Texas J Sci. 1961;8:231–4.

14. Yuvraj Sh, Lin F-Y, Chang T-Hl, Yeh C-T. Thermal decomposition of metal nitrates in air and hydrogen environments. J Phys Chem B. 2003;107:1044–7.

15. Komissarova LN. Inorganic and analytical chemistry of scandium. Moscow: URSS; 2001.

16. Stünzi H, Marty W. Early stages of chromium(III) hydrolysis in aqueous solution. 1. Characterization of tetrameric species. Inorg Chem. 1983;22:2454–61.

17. Rao JR, Gayatri R, Rajaram R, Nair BU, Ramasami T. Chromium(III) hydrolytic oligomers: their relevance to protein binding. Biochim Biophys Acta. 1999;1492:595–602.

18. Speight J. Lange's handbook of chemistry, 16th ed. McGrow-Hill, 1999.

19. Gray RJ. The normal oxidation-reduction potentials of the system hexavalent-trivalent chromium-tetravalent chromium. PhD Thesis, Faculty of Pure Science, Columbia University. N.Y. 1940.

20. Rao CNR, Rao GVS, Transition metal oxides. Crystal chemistry, phase transition and related aspects, U.S. Department of Commerce, National Bureau of Standards, U.S. Government Printing Office. Washington, 1974.

21. Wells AF. Structural Inorganic Chemistry. 5th ed. London: Clarendon, Oxford University Press; 1984.

22. Hammond Ch. The Basics of crystallography and diffraction. 3rd ed. London: Oxford University Press; 2009.